

# THERMODYNAMIC, PHASE EQUILIBRIUM, AND CRYSTAL CHEMICAL BEHAVIOR IN THE NEPHELINE–KALSILITE SYSTEM

GUY L. HOVIS\*, ANDREW MOTT\*\*, and JACQUES ROUX\*\*\*

**ABSTRACT.** Reversed phase equilibria have been determined from 500 to 1050 °C along the nepheline–kalsilite solvus for crystalline solutions having 12.5 mole percent excess Si relative to stoichiometric Al:Si = 1:1. The resulting 961 °C critical temperature ( $T_c$ ) for this high-Si series is substantially lower than those (1108 and 1265 °C) of two previously studied series containing less Si. Hydrofluoric acid solution calorimetric data collected at 50 °C for mid-compositional members of this high-Si series show positive enthalpies of mixing ( $H_{ex}$ ) that are lowest in magnitude among the three series, correlating well with the lower  $T_c$ . The thermodynamic and phase behavior of minerals in the nepheline–kalsilite system are related to structural strain associated with the entrance of  $K^+$  into the smaller of nepheline’s two alkali crystallographic sites and also by equilibrium between minerals with related, yet distinct, structures. Positions of the sodic limbs of the solvi are governed in part by the preference of nepheline’s large hexagonal alkali site for vacancies (instead of sodium) near room temperature, with an apparent switch to preference for  $K^+$  at  $T \geq 500$  °C. Positions of the potassic limbs of the solvi are governed only by the substitution of relatively small  $Na^+$  into the ditrigonal site of kalsilite, which is accompanied by ideal thermodynamic behavior of the solution calorimetric data. The collective structural and crystal chemical distinctions among the various members of these crystalline solutions produce differences in thermodynamic behavior and miscibility that are substantial for the modest observed differences in system chemistry.

## INTRODUCTION

### *Previous Work*

Research reported by Hovis and others (1992) and Hovis and Roux (1993) described two nepheline–kalsilite solid solution series that differed from one another in several respects. The so-called “synthetic” series, made by K-Na ion exchange of sodic nepheline hydrothermally synthesized from gel (Hamilton and Henderson, 1968), contained just 1.7 mole percent excess silicon above the nominal Al:Si of 1:1,  $(Na,K)_{0.983}[ ]_{0.017}Al_{0.983}Si_{1.017}O_4$  (where  $[ ]$  represents vacancies). The “natural” series was produced by ion-exchange of a natural Monte Somma nepheline specimen with composition  $Na_{0.747}Ca_{0.036}K_{0.129}[ ]_{0.088}Al_{0.948}Si_{1.052}O_4$  that contained 5.2 percent excess silicon and 3.6 mole percent Ca. Although specimens across each series had constant excess Si, the “natural” series varied systematically from the nepheline parent to the Na-free end member not only in Na:K ratio but also in Ca and vacancy content due to  $[ ]Ca^{2+} = 2K^+$  ion exchange during synthesis. This resulted in a potassic end-member of composition  $K_{0.948}[ ]_{0.052}Al_{0.948}Si_{1.052}O_4$ .

Hovis and Roux (1993) reported solution calorimetric results for members of these series. The data showed that enthalpies of K-Na mixing were distinctly greater for the natural than for the synthetic series. The substantial energetic effect of excess Si on both end-member enthalpies and thermodynamic mixing properties suggested that investigation of the nepheline–kalsilite solvus would be worthwhile. (We use the term “solvus” here, even though coexisting minerals on either side of the miscibility gap have distinct, although related, structures.) In addition, excess Si in such feldspathoids

\*Department of Geology and Environmental Geosciences, Lafayette College, Easton, Pennsylvania 18042, USA; hovisguy@lafayette.edu

\*\* Department of Geological and Environmental Sciences, Stanford University, Stanford, California 94305, USA

\*\*\* Physique des Minéraux et des Magmas, IPGP, 4 place Jussieu, 75252 Paris cedex 05, France

has been shown to be petrologically significant (for example, Hamilton and MacKenzie, 1960; Henderson and Gibb, 1983). The rapid diffusion of  $\text{Na}^+$  and  $\text{K}^+$  in these minerals at temperatures as low as 400 and 500 °C during earlier high-temperature X-ray diffraction measurements (Crelling and Hovis, 1996; Hovis and others, 2003, 2006) bode well for the achievement of chemical equilibrium in such a study. As a result Hovis and Crelling (2000) successfully investigated both solvi, and determined critical temperatures of 1108 °C and 1265 °C for the synthetic and natural series, respectively. The higher  $T_c$  of the natural series was consistent with the greater enthalpies of mixing measured for that series. The connection between thermodynamic data and solvus characteristics, including recognition of the substantial effect of excess Si on these properties, added to the earlier pioneering work on the solvus by Tuttle and Smith (1958) and Ferry and Blencoe (1978).

### *Synthesis of High-Si Nepheline–Kalsilite Crystalline Solutions*

Na-free kalsilite end-members for the natural and synthetic series were produced through multiple ion-exchange experiments of the original parent nepheline specimens in molten KCl. Compositionally intermediate series members were made by annealing carefully weighed powders of the nepheline and kalsilite end members to produce desired bulk compositions. The well-mixed powders generally were held at temperatures above the solvus, quenched, and remixed at 24- to 48-hour intervals to promote alkali homogenization (details in Hovis and Roux, 1993). Successful syntheses produced sharp X-ray powder diffraction maxima for the resulting materials, as opposed to doubled or broadened peaks characteristic of inhomogeneous samples.

Several years after the initial calorimetric investigation of these two series Roux succeeded in synthesizing a highly silicic nepheline end-member containing 12.5 mole percent excess Si,  $\text{Na}_{0.875}[\text{Al}_{0.125}\text{Al}_{0.875}\text{Si}_{1.125}\text{O}_4]$ . As before, a Na-free kalsilite end-member was produced by K-exchange of the parent nepheline in molten KCl (Hovis and Roux, 1999). Given previous results (Hovis and Roux, 1993; Hovis and Crelling, 2000) it was our expectation that a high-Si series would be associated with the highest critical temperature among the three series. In an attempt to synthesize intermediate K-Na compositions for calorimetric investigation, therefore, annealing was attempted at 1300 °C and above. This had the effect of increasing the difficulty of cooling the run products quickly enough through subsolvus conditions to prevent exsolution during the quench. It also resulted in the production of small amounts of leucite as a byproduct in some of the K-Na homogenization experiments, and the partial melting of samples in others. We were successful, however, in producing high-quality samples along the flanks of the solvus, where annealing could be conducted at lower temperatures. This explains limitation of previously synthesized “high-Si series” members to four Na-rich nepheline samples containing up to 15.4 mole percent K and three K-rich kalsilite samples having up to 13.7 mole percent Na (Hovis and Roux, 1999).

Despite the earlier difficulties, investigation of a high-Si solvus seemed worthwhile as an attempt to understand why earlier mid-composition syntheses had been unsuccessful, and also to further understand the energetic and phase-equilibrium consequences of excess-Si substitution. We report the new results in this paper.

## COMPONENTS AND STRUCTURES

### *Chemical Components*

In our previous research (Hovis and Roux, 1993, 1999; Hovis and Crelling, 2000) four chemical components were utilized to describe the compositions of nepheline–kalsilite minerals. These included Ne ( $\text{NaAlSiO}_4$ ), Ks ( $\text{KAlSiO}_4$ ), 2Qz ( $[\text{Si}_2\text{O}_4]$ ), and 0.5An ( $[\text{Ca}_{0.5}\text{AlSiO}_4]$ ), where, for example,  $X_{\text{Ne}}$  indicates the mole fraction of Ne. Although neither the high-Si series discussed here nor the synthetic series of Hovis and

Roux (1993) contain Ca, the 0.5An component was included because of its presence in natural series members.

Mole fractions (X) of species occupying the alkali site(s) of nepheline–kalsilite minerals,  $\text{Na}^+$ ,  $\text{K}^+$ ,  $\text{Ca}^{2+}$ , and vacancies (henceforth Vac), are directly related to mole fractions of the chemical components as

$$X_{\text{Na}} = X_{\text{Ne}}, \quad X_{\text{K}} = X_{\text{Ks}}, \quad X_{\text{Ca}} = 0.5 X_{0.5\text{An}}, \quad \text{and} \quad X_{\text{Vac}} = X_{2\text{Qz}} + 0.5 X_{0.5\text{An}} \quad (1-4)$$

such that

$$X_{\text{Na}} + X_{\text{K}} + X_{\text{Ca}} + X_{\text{Vac}} = X_{\text{Ne}} + X_{\text{Ks}} + X_{0.5\text{An}} + X_{2\text{Qz}} \quad (5)$$

Because of the relatively small amounts of  $\text{Ca}^{2+}$  in the natural series and also the similar sizes of  $\text{Na}^+$  and  $\text{Ca}^{2+}$ ,  $X_{\text{Na}}$  and  $X_{\text{Ca}}$  will be combined here to form a single variable, as in Hovis and Roux (1993). Thus,

$$X_{\text{Na(revised)}} = X_{\text{Ne(original)}} + 0.5 X_{0.5\text{An}} = X_{\text{Na(original)}} + X_{\text{Ca}} \quad (6)$$

which henceforth we shall call simply  $X_{\text{Na}}$ . With this adjustment, then

$$X_{\text{K}} + X_{\text{Na}} + X_{\text{Vac}} = 1 \quad (7)$$

#### *Mineral Structures*

Mineral structures in the nepheline–kalsilite system have been investigated extensively (Buerger and others, 1954; Hahn and Buerger, 1955; Smith and Tuttle, 1958; Perotta and Smith, 1965; Dollase and Peacor, 1971; Benedetti and others, 1977; Dollase and Freeborn, 1977; Dollase and Thomas, 1978; Stebbins and others, 1986; Hippler and Bohm, 1989; Capobianco and Carpenter, 1989; and Carpenter and Cellai, 1996). The various atomic arrangements are stuffed derivatives of tridymite that differ from each other in the details of framework configuration, as well as the number and kinds of alkali sites (see summary of Merlino, 1984). Hovis and Roux (1993, 1999; also Hovis and others, 1992) encountered phases at room temperature having one of three structures: nepheline, tetrakalsilite (or panunzite), and kalsilite. Nepheline itself, which has a small oval and a larger hexagonal alkali site with molar oval:hexagonal ratio of 3:1, can be divided into two compositional regions. One of these we shall call “Na-nepheline” (at  $X_{\text{Na}} \geq 0.75$ ) in which it is likely that only Na ( $\pm \text{Ca} \pm \text{vacancies}$ ) occupies the smaller alkali site. “K-nepheline” will apply to compositions where K occupies a portion of the smaller sites. Hovis and others (1992) have stated that vacancies in nepheline seem to prefer the larger alkali site in nepheline, which agreed with the observations of Buerger and others (1954) and Barth (1963). Results from the current study lead to further refinement of this point. Once K enters the smaller alkali site, linear trends of unit-cell parameters ( $a$ ,  $c$ , volume) change slope on plots against composition (figs. 2, 3 and 4 of Hovis and others, 1992; also Smith and Tuttle, 1957; Donnay and others, 1959; and Ferry and Blencoe, 1978). K-nepheline thus behaves somewhat differently than its sodic analog.

By contrast with nepheline, K-rich kalsilite has only one type of alkali site, ditrigonal in geometry and different from either of the alkali sites in nepheline. Tetrakalsilite has all three types of alkali sites found in the other two structures. Merlino (1984), however, apparently errs in his table IV, where it is indicated that the ratio of hexagonal:ditrigonal:oval sites is 2:12:18, whereas a ratio of 2:18:12 correlates correctly with his figure 8 of the tetrakalsilite structure. If one assumes that  $\text{K}^+$  prefers the hexagonal and ditrigonal sites and  $\text{Na}^+$  the oval site of the structure, this predicts an ideal tetrakalsilite composition (if Al:Si is 1:1) of  $\text{K}_{0.625}\text{Na}_{0.375}\text{AlSiO}_4$  (as opposed to  $\text{K}_{0.438}\text{Na}_{0.562}\text{AlSiO}_4$ ). This is only slightly less potassic than tetrakalsilite compositions synthesized by this laboratory in earlier studies (table 1 of Hovis and others, 1992).

## EXPERIMENTAL TECHNIQUES

*Solvus Experiments*

In order to achieve reversed chemical equilibrium along the solvus of the high-Si series experiments of two types were conducted. In one case sodic nepheline (sample 9504) and kalsilite (sample 9507) powders were carefully weighed on a Mettler AT201 balance in order to achieve a desired bulk composition, then thoroughly mixed on weighing paper, transferred to a 1-cm diameter cylindrical platinum crucible and compressed using a bent spatula. The covered crucible was placed in a furnace preheated to the desired temperature (T). At run conditions the sodic and potassic grains exchanged ions (nepheline becoming more potassic and kalsilite becoming more sodic), shown well on a T-X diagram where they approach their final compositions from the “outside” of the solvus “inward”. These experiments are designated O-I (outside-in) or “homogenization” experiments. At the conclusion of an experiment the crucible was removed as rapidly as possible from the furnace, and its base quenched in ice water.

In the second case powders from homogenization experiments with documented pairs of coexisting phases were returned to the preheated furnace at a temperature 50 to 100 °C below that of the previous annealing. Quench was the same as for O-I experiments. In this case compositions of the coexisting phases moved further apart relative to the previous compositional pair, Na-rich phases becoming more sodic and K-rich phases becoming more potassic, thereby approaching the solvus from the “inside outward” (henceforth I-O experiments). Compositions of the newly equilibrated phases were compared with results from O-I experiments conducted at the same temperature. Results imply that chemical equilibria were indeed reversed.

*X-Ray Powder Diffraction Measurements*

The products of all solvus experiments were characterized by X-ray diffraction (Scintag PAD-V DMS 2000 system) using filtered Cu radiation and a solid state detector.  $\text{CuK}_{\alpha 2}$  peaks were stripped mathematically using Scintag software. Diffraction angles ( $2\theta$ ) were determined by Scintag’s Peakfinder program. Chemical compositions of the products were determined from the  $2\theta$  positions of the compositionally-sensitive (201)/(101) peak for K-nepheline or kalsilite, respectively (different Miller indices being the result of the doubled  $a$  crystallographic axis of nepheline relative to kalsilite). Data for these peaks are shown in figure 1, along with (401) data for tetrakalsilite (with a quadrupled  $a$  axis relative to kalsilite) for the natural and synthetic series. For the high-Si series “tetrakalsilite” data are actually for an unidentified phase having an X-ray pattern similar to that of tetrakalsilite, but with additional peaks relative to the latter; this could be a phase similar to the pseudohexagonal kalsilite described by Capobianco and Carpenter (1989). Relevant equations for each room-temperature compositional region of the high-Si series are given in table 1. Similar equations for the synthetic and natural series are given in table 1 of Hovis and Crelling (2000). Two equations are given for the K-nepheline segment of the high-Si series; the first (dashed line in fig. 1) is based on five K-nepheline compositions for that series (excluding calorimetric sample 0805, which was produced late in the investigation), even though the two most potassic samples in that segment (0707 and 0709/0717) had X-ray patterns with three low-intensity peaks attributed to the highest intensity peaks of leucite. The second equation (solid line in fig. 1) is based on the three sodic K-nepheline members (again excluding 0805), none of which showed leucite peaks. Comparison of the two lines shows that use of these alternative equations gives compositions different by as much as 0.02  $X_{\text{K}+\text{Vac}}$  only for K-nepheline specimens where  $X_{\text{K}+\text{Vac}} > 0.62$ . This would affect composition determination of the K-nepheline phase only for run temperatures above 920 °C. The final data show, however, that

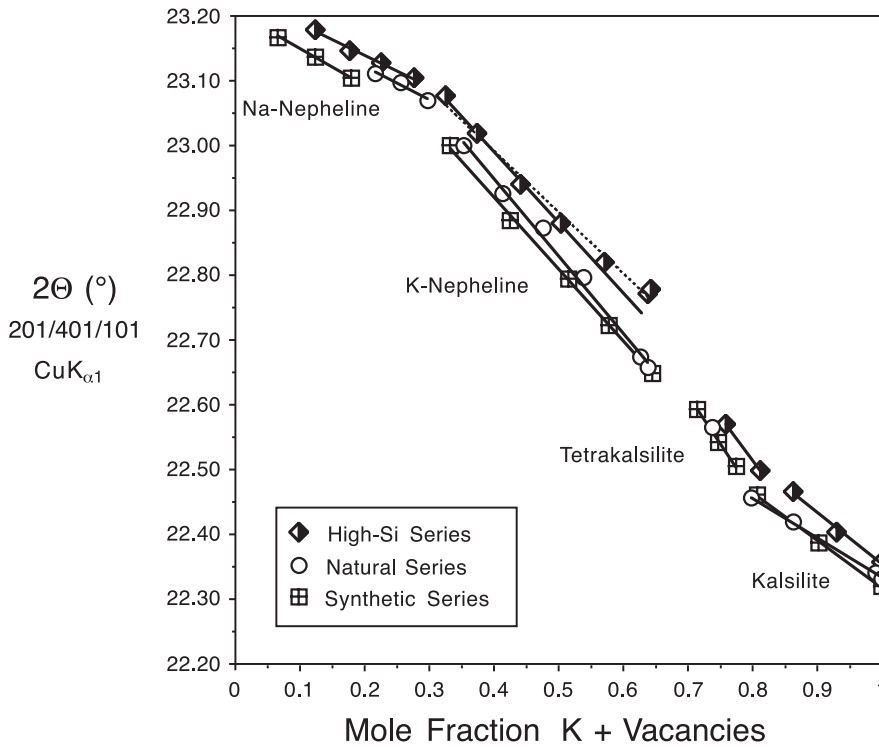


Fig. 1. Variation of  $2\theta$  ( $\text{CuK}_{\alpha 1}$  radiation,  $\lambda = 1.54056 \text{ \AA}$ ) for the (201)/(401)/(101) peak of nepheline/tetrakalsilite/kalsilite, respectively. The two fits to the K-nepheline segment of the high-Si samples are discussed in the text. The region labeled “tetrakalsilite” for the high-Si series is actually a tetrakalsilite-like phase with an X-ray pattern similar but not identical to the former.

results at such temperatures are in good continuity with those from lower-temperature experiments. Previous solvus work by Hovis and Crelling (2000) showed that chemical compositions estimated using the (201)/(401)/(101) peak were in good agreement (within  $X_{\text{K+vac}}$  of 0.02 in 72% of the cases and within 0.03 in all cases) with direct electron microprobe data for coexisting phases. There is no evidence that the presence of leucite adds noticeably to the overall uncertainty of solvus compositions for the high-Si series.

A second issue that arises is whether the phases from the various experiments coexist as coherent or incoherent entities. If coherent, then equations based on

TABLE 1  
Equations for  $2\theta$  of the (201) peak for the high-Si nepheline–kalsilite series

Compositional Region	Coefficients for linear equations*	
	Intercept	Slope
Na-Nepheline	23.233	-0.47962
K-Nepheline (all samples except 0805)	23.339	-0.89487
K-Nepheline (four most sodic samples excluding 0805)	23.417	-1.0747
Tetrakalsilite-like phase	23.523	-1.2635
Kalsilite	23.147	-0.79534

\* Where  $2\theta$  (°) = Intercept + Slope \*  $X_{\text{K+vac}}$ , for  $\text{CuK}_{\alpha 1}$  radiation,  $\lambda = 1.54056 \text{ \AA}$ .

chemically homogeneous single-phase specimens would not be appropriate for run products consisting of strained coexisting phases. There are two pieces of evidence, however, which indicate that coexisting phases are not likely to be coherent. Electron microprobe evidence of chemically distinct whole grains for homogenization runs in the previous solvus study (Hovis and Crelling, 2000) points to incoherency of experimental products, as individual whole grains tended to be either relatively potassic or relatively sodic, rather than coexistences of Na-rich and K-rich areas within the same grain. Secondly, at many temperatures the compositions determined for O-I experiments agreed nearly perfectly with the reversed I-O data. This implies that the corresponding I-O samples are incoherent as well.

Unit-cell parameters were refined from X-ray powder diffraction data using the software of Holland and Redfern (1997). Angles  $2\theta$  ( $\text{CuK}_{\alpha 1} \lambda = 1.54056 \text{ \AA}$ ) were corrected manually relative to a silicon internal standard (NBS SRM 640a) with a unit-cell dimension of  $5.430825 \text{ \AA}$ .

Solution Calorimetry

Determination of the high-Si series solvus enabled synthesis of calorimetric samples at intermediate K:Na ratios, where previous synthesis attempts had been unsuccessful (Hovis and Roux, 1999). This was accomplished by the method described above for intermediate members of the synthetic and natural series. Temperatures and times for the various samples are recorded in table 2. Calorimetric measurements were made on six high-Si samples in the K-nepheline compositional range.

The calorimetric system used to measure enthalpies of solution has been described in Hovis and Roux (1993) and Hovis and others (1998). Because sample availability was highly limited, most calorimetric experiments were conducted on sample quantities of  $\sim 25 \text{ mg}$  (although  $45 \text{ mg}$  for sample 0805), with at least two experiments for each sample. Note that samples 0709 and 0717 are essentially the same, with extended annealing for 0717. Specimens were dissolved in  $910.1 \text{ g}$  (about one liter) of  $20.1 \text{ weight percent}$  hydrofluoric acid (HF) at  $49.96 \pm 0.02 \text{ }^\circ\text{C}$  under isoperibolic conditions (that is, the temperature of the water bath surrounding the calorimeter was held constant) utilizing an internal sample container (Waldbaum and Robie, 1970). Either one or two solution calorimetric experiments were performed in each liter of acid. Multiple dissolutions in the same solution had no detectable effect on the data because of the high dilution of dissolved ions. Because these samples dissolved rapidly (generally in less than 3 minutes), the calorimetric experiments were conducted on powders, but not ultrafine material; this avoided the possibility of heat effects associated with extremely small grain sizes (Nitkiewicz and others, 1983).

TABLE 2  
*Annealing conditions for calorimetric samples*

Sample Number	X <sub>K+Vac</sub>	Temperature(s) (°C)	Hours
0805	0.326	744 ± 5	72.1
0705	0.376	751 ± 2	72.7
0704	0.440	945 ± 2	73.6
0716	0.506	895 ± 5	72.0
0707	0.572	1017 ± 3	47.0
0709	0.639	751 ± 2, 995 ± 2, 1024 ± 2	47.5, 25.5, 17.4
0717	0.639	sample 0709 plus 1067 ± 2, 1053 ± 2	sample 0709 plus 4.0, 16.0

For samples 0709 and 0717 there is a sequential correspondence among the various temperatures and times.



## RESULTS

*Solvus Reversals*

The results of solvus experiments for high-Si nepheline–kalsilite samples are recorded in table 3 and shown in figure 2. Because there are three occupants in the alkali sites, two of these ( $X_K$  and  $X_{Vac}$ ) have been combined in figure 2 as the compositional parameter, leaving  $X_{Na}$  as the remaining compositional variable. Note that O-I and I-O results at most temperatures are the same within the uncertainty of compositional determination. Even at temperatures as low as 400 and 500 °C compositions of the coexisting phases evidence a close approach to reversed chemical equilibrium.

Figure 3A is a comparison of high-Si solvus data to those for the synthetic and natural series from the earlier work of Hovis and Crelling (2000), utilizing  $X_{K+Vac}$  to represent composition. It is perhaps best initially to compare data of the synthetic and high-Si series, between which the only difference is excess Si content of 1.7 versus 12.5 mole percent, respectively. Although the sodic limb of the solvus for the high-Si series is shifted relative to low-Si samples, the two series essentially parallel one another below

TABLE 3  
*Results of solvus experiments*

Experiment Number	Temperature (°C)	2 $\Theta$ Na-rich Phase(201)	Calculated Mole Fraction K in Na-rich Phase*	Calculated Mole Fraction Na in Na-rich Phase*	2 $\Theta$ K-rich Phase (101) or (401)	Calculated Mole Fraction K in K-rich Phase*	Calculated Mole Fraction Na in K-rich Phase*
<b>"Inside-Out" (Exsolution) Experiments</b>							
0612	801	22.850	0.403	0.472	22.494	0.696	0.180
0618	801	22.837	0.415	0.460	22.504	0.684	0.192
0625	902	22.770	0.477	0.398	22.550	0.626	0.249
0626	801	22.842	0.410	0.465	22.501	0.687	0.189
0627	502	22.983	0.279	0.596	22.402	0.812	0.064
0630	700	22.925	0.333	0.542	22.479	0.715	0.161
0631	601	22.948	0.311	0.564	22.427	0.780	0.096
0650	976	22.694	0.548	0.327	22.650	0.566**	0.309**
0651	950	22.708	0.535	0.340	22.651	0.566**	0.309**
0653	752	22.866	0.387	0.488	22.501	0.687	0.189
0655	652	22.941	0.318	0.557	22.431	0.775	0.100
0656	553	22.988	0.274	0.601	22.411	0.801	0.075
<b>"Outside-In" (Homogenization) Experiments</b>							
0617	876	22.809	0.441	0.434	22.534	0.646	0.230
0621	801	22.862	0.391	0.484	22.507	0.680	0.195
0622	900	22.781	0.467	0.408	22.563	0.610	0.265
0628	601	22.951	0.309	0.567	22.432	0.774	0.101
0629	700	22.909	0.348	0.527	22.453	0.748	0.128
0632	950	22.748	0.497	0.378	22.629	0.527	0.349
0638	950	22.717	0.526	0.349	22.649	0.567**	0.308**
0654	751	22.868	0.386	0.489	22.493	0.697	0.178
0657	500	23.023	0.242	0.633	22.396	0.820	0.055
0658	553	22.996	0.267	0.608	22.396	0.819	0.057
0659	652	22.973	0.289	0.586	22.439	0.765	0.111

\* Mole fraction vacancies in all samples is assumed to be 0.125. All compositions are relative to 4 oxygen ions.

\*\* K-rich phase is tetrakalsilite-like phase; kalsilite is K-rich phase for all other experiments.

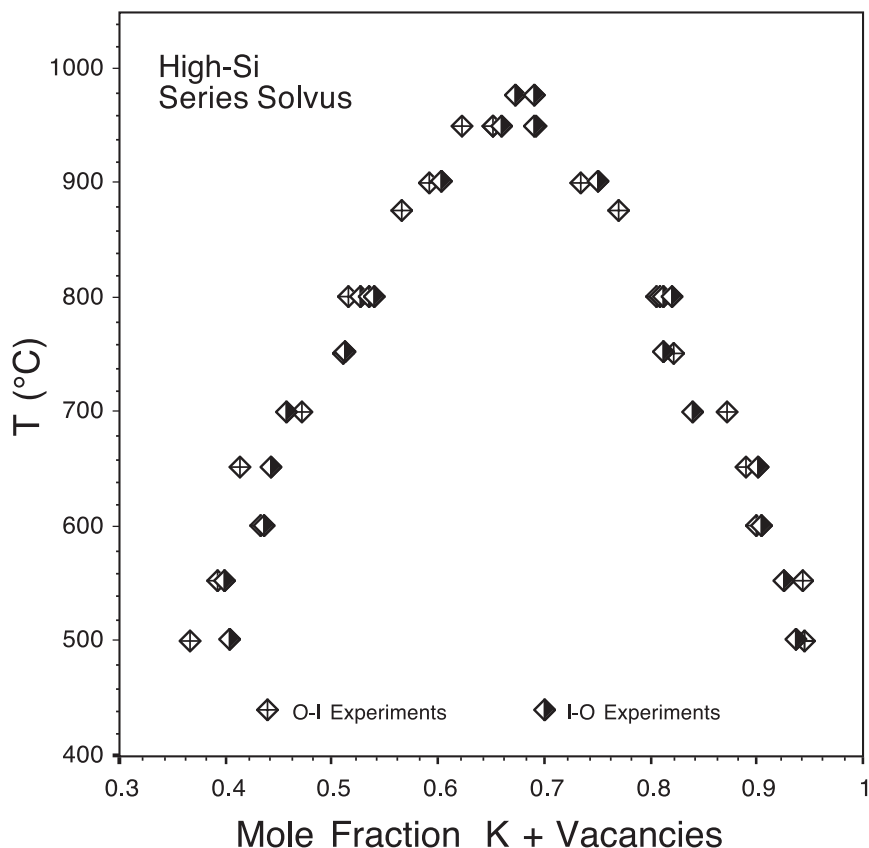


Fig. 2. Results of solvus experiments for the high-Si nepheline–kalsilite series. Half-filled diamonds are for “inside-out” (exsolution) experiments, whereas diamonds with crosses are for “outside-in” (homogenization) experiments. Compositions were estimated from the (201) X-ray data shown in figure 1.

800 °C. The compositional difference between the two is mostly vacancy, not K, content. This is shown well in figure 3B, where  $X_K$  alone is used as the compositional parameter. The latter portrayal also shows that all three solvi converge toward a common  $X_K$  content of  $\sim 0.25$  at temperatures approaching 500 °C.

When  $X_{K+Vac}$  is utilized as the compositional parameter (fig. 3A), the potassic limbs of the three solvi are essentially coincident below 900 °C. All potassic limbs, therefore, have common Na ( $\pm$ Ca) content below this temperature, approaching  $\sim 6$  mole percent Na (94 mol % K + Vac) at 500 °C.

Among the various nepheline–kalsilite series the high-Si solvus has a distinctly lower  $T_c$  than the nearly stoichiometric synthetic series. Curiously, even though the natural series has intermediate Si content relative to other series, it displays the highest  $T_c$ . The sodic limb of the natural series does indeed cross that of the synthetic series with decreasing temperature (fig. 3A), occupying an intermediate compositional position relative to the other series at lower temperatures, as one might expect.

It is possible to determine the critical temperature of a solvus precisely using a plot of inverse absolute temperature [ $1/T(K)$ ] against  $(\text{arctanh } s)/s$  (Thompson and Waldbaum, 1969a, 1969b), where  $s$  is the compositional difference between a pair of coexisting phases at a given temperature and  $\text{arctanh } s$  is the hyperbolic arctangent of  $s$ .



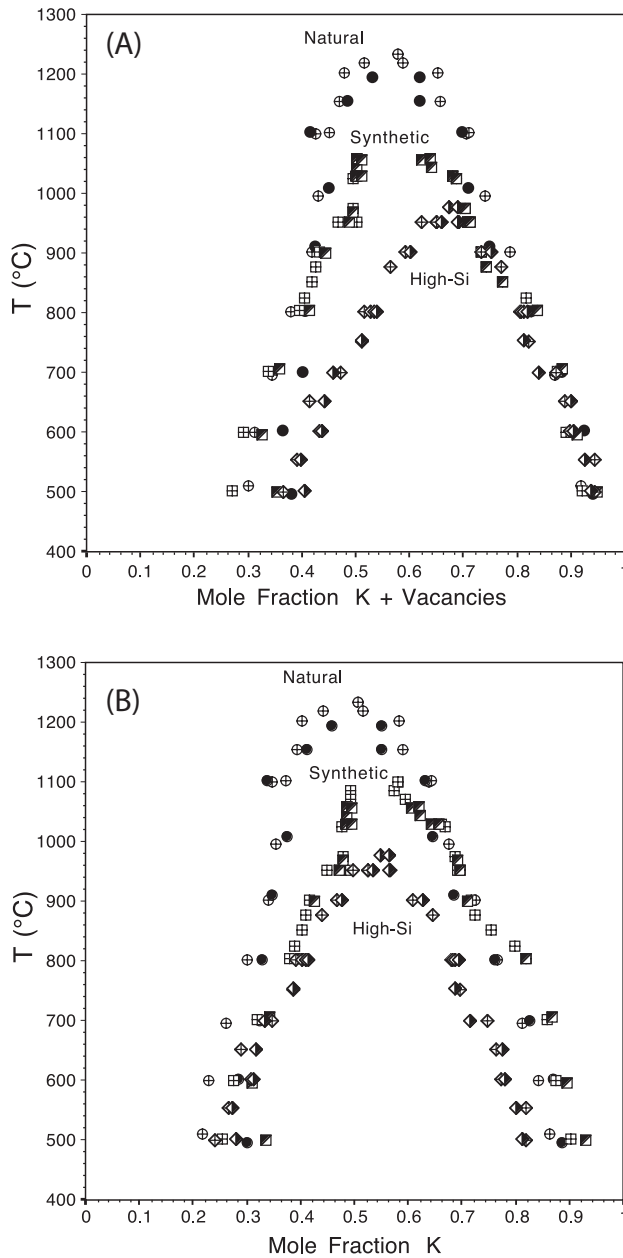


Fig. 3. (A) Comparison among solvus data for three nepheline–kalsilite series based on the current investigation as well as the data of Hovis and Crelling (2000). Symbols for the synthetic, natural, and high-Si series are squares, circles, and diamonds, respectively. Entirely- or partially-filled symbols are for “inside-out” (exsolution) experiments, whereas symbols with crosses are for “outside-in” (homogenization) experiments. Compositions were estimated from the (201)/(401)/(101) X-ray peaks shown in figure 1. If utilizing  $X_{\text{K}+\text{Vac}}$  as the compositional parameter, the other compositional parameter is  $X_{\text{Na}}$ . Note the overlap of the potassic limbs of all three solvi. (B) Same as figure 3A except using  $X_{\text{K}}$  as the compositional parameter. The other compositional parameter, therefore, is  $X_{\text{Na}+\text{Vac}}$ . Note the convergence of the sodic limbs of all three solvi to the  $X_{\text{K}} = 0.25$  composition.

$\{= 0.5 \ln [(1 + s)/(1 - s)]\}$ .  $T_c$  is reached when estimated from the value of inverse temperature where  $(\operatorname{arctanh} s)/s$  extrapolates to a value of 1.0 [as in fig. 5 of Hovis and Crelling (2000) for the synthetic and natural series]. Data in figure 4 show a good linear fit to solvus data at temperatures of 750 °C (1023 K) and above (that is,  $1/T(K) < 0.0009775$ ). The calculated  $T_c$  for the high-Si series is 1234 K (961 °C), compared with the previously determined critical temperatures of 1108 and 1265 °C for the synthetic and natural series, respectively. The lower  $T_c$  of the high-Si series thus contradicts our previous expectation that increased excess Si raises  $T_c$  (Hovis and Crelling, 2000). Still, the 304 °C difference among the critical temperatures of the three series emphasizes the substantial differences in phase behavior among the series.

*X-Ray and Unit-Cell Data*

Unit-cell dimensions for the newly synthesized high-Si calorimetric samples are given in table 4. Plots of unit-cell parameters  $a$ ,  $c$  and volume against composition (figs. 5, 6, and 7) show discontinuities that are similar, though displaced, relative to those of previously-studied series. The slopes of these parameters with  $X_{K+Vac}$  (or  $X_K$ ), particularly in the K-nepheline compositional range, show slightly different trends than for the synthetic and natural series (Hovis and others, 1992). Unfortunately, synthesis attempts at  $X_{K+Vac}$  values of 0.813, 0.758, and 0.689 resulted in a phase (or phases) having X-ray patterns that, although similar to those of other phases in the system

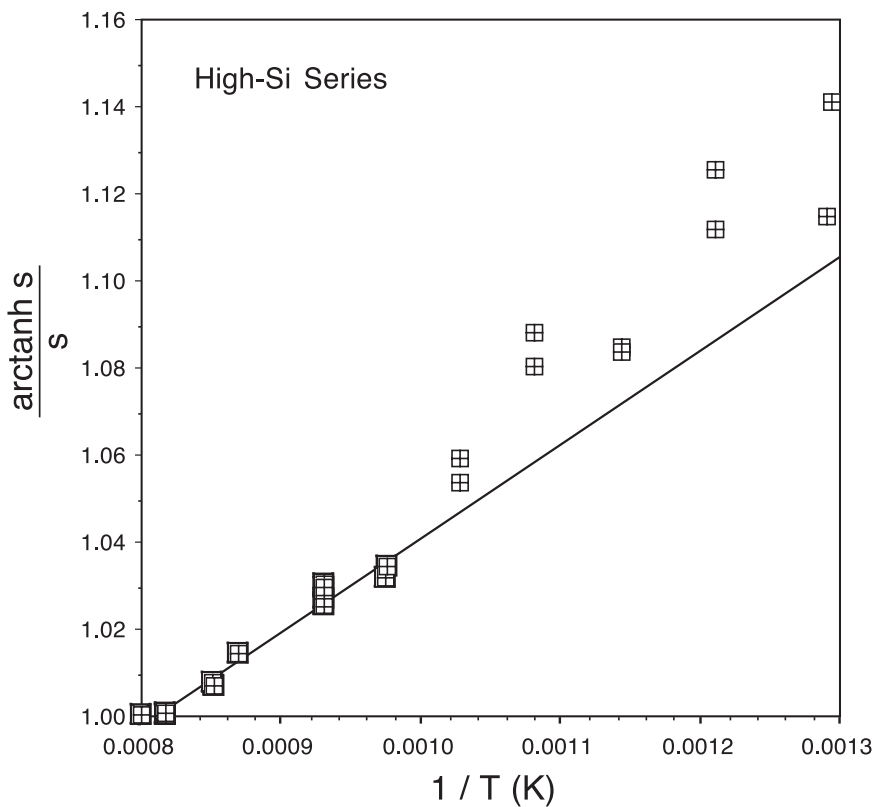


Fig. 4. Plot of the  $(\operatorname{arctanh} s)/s$  against inverse temperature (K) for the high-Si series, where  $\operatorname{arctanh} s = \{0.5 \ln [(1 + s)/(1 - s)]\}$  and  $s$  is the compositional difference between a compositional pair along the solvus. This function approaches a value of 1.0 at the critical temperature (Thompson and Waldbaum, 1969a, 1969b). Only the bold data points were used in the linear fit.

TABLE 4  
Unit-cell dimensions and position of the (201) peak for calorimetric samples

Sample Number	Mole Fraction K	Mole Fraction Na	Mole Fraction Vacancies	a (Å)	c (Å)	Unit-Cell Volume (Å <sup>3</sup> )	2Θ (°) for (201) (λ = 1.54056 Å)
0805	0.201	0.674	0.125	10.0104 (06)	8.3811(09)	727.33(10)	23.073
0705	0.251	0.625	0.125	10.0350 (06)	8.3949(10)	732.12(10)	23.016
0704	0.315	0.560	0.125	10.0698 (09)	8.4128(12)	738.77(14)	22.938
0716	0.381	0.494	0.125	10.0960 (07)	8.4228(09)	743.51(11)	22.893
0707	0.447	0.428	0.125	10.1307 (12)	8.4379(16)	749.98(18)	22.817
0709	0.514	0.361	0.125	10.1564 (20)	8.4511(21)	754.97(31)	22.764
0717	0.514	0.361	0.125	10.1546 (12)	8.4588(15)	755.37(19)	22.768

Numbers in brackets are standard errors (1 s) in the last two decimal places of each parameter. Compositions are per 4 oxygen ions.

(especially tetrakalsilite), were unidentifiable. The most potassic K-nepheline samples (0707 and 0709/0717) for which calorimetric data are reported ( $X_{K+Vac} = 0.572$  and 0.639, respectively) show signs of minor breakdown by the inclusion of three low-

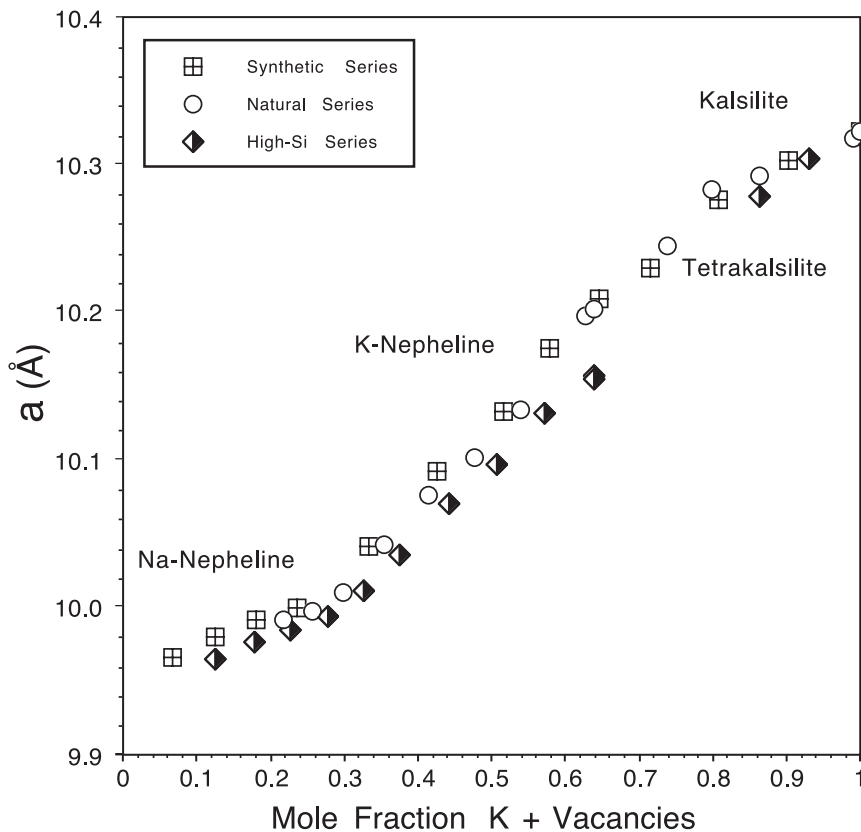


Fig. 5. Plot of the  $a$  unit-cell dimension against  $X_{K+Vac}$  for three nepheline–kalsilite series. Note the new data for K-nepheline specimens of the high-Si series; other data come from Hovis and others (1992) and Hovis and Roux (1999). The only tetrakalsilite specimens among the three series are represented by the two data points to the immediate left of “Tetrakalsilite” labeling. For comparison with nepheline data,  $a$  values for kalsilite are doubled and those of tetrakalsilite are halved.

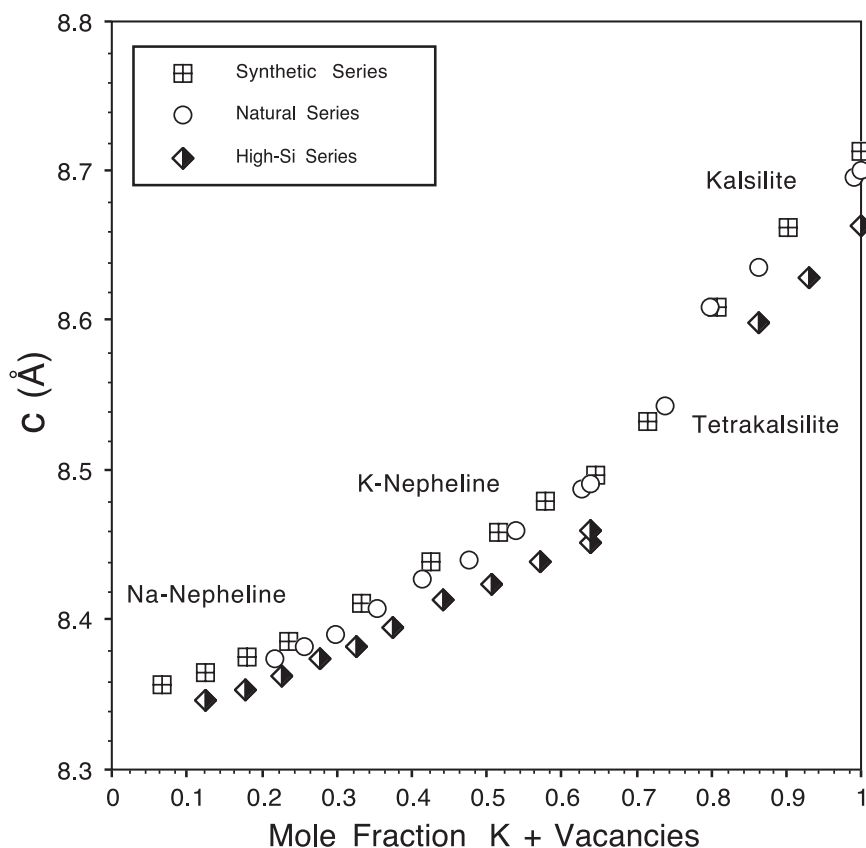


Fig. 6. Plot of the  $c$  unit-cell dimension against  $X_{K+Vac}$  for three nepheline–kalsilite series.

intensity X-ray peaks corresponding to the highest-intensity peaks of leucite. A least-squares fit of K-nepheline volume data for the four most sodic K-nepheline members (including 0805) of the high-Si series gives a very similar relationship to that when volume data at all six compositions are utilized, thus different trends for the high-Si K-nepheline samples do seem to represent a real difference between this and previously studied series (Hovis and Roux, 1993, 1999).

As noted, the X-ray pattern for the unknown room-temperature quench product of samples at  $X_{K+Vac}$  values of 0.689, 0.758, and 0.813 was similar to those of other minerals in this system. Indeed, it was possible to identify a peak corresponding to the compositionally-sensitive (201)/(401)/(101) of nepheline/tetrakalsilite/kalsilite. Values of  $2\theta$  for this peak (shown for the high-Si series in the tetrakalsilite region of fig. 1) were utilized in composition determination for solvus experiment 0628, in which the same phase was detected.

#### Solution Calorimetric Results

The enthalpies of solution for K-nepheline samples of the high-Si series are recorded in table 5. Figure 8 shows the negatives of the average heats of solution ( $-H_{soln}$ ) for each of these samples with generalized standard deviations ( $\pm 0.4\%$  of the heats of solution) based on the precision of all calorimetric data. It also includes comparative data for the synthetic and natural series from Hovis and Roux (1993) plus

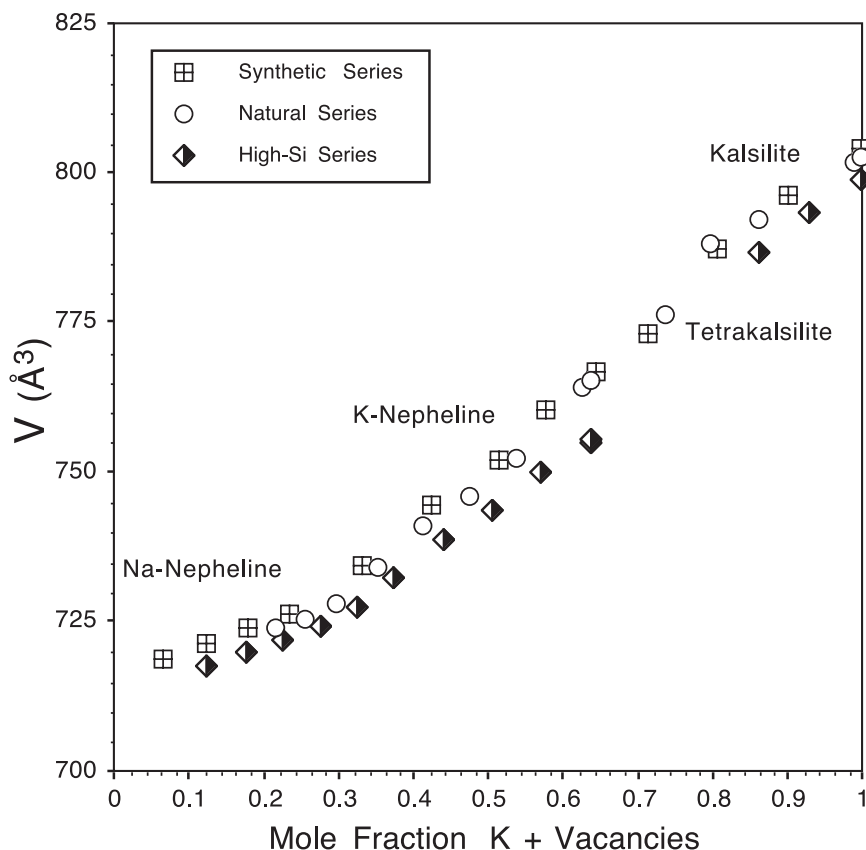


Fig. 7. Plot of unit-cell volume against  $X_{K+Vac}$  for three nepheline–kalsilite series. For comparison with nepheline data, volume values for kalsilite are quadrupled and those of tetrakalsilite are one-quarter those of actual values.

data for earlier high-Si Na-nepheline and kalsilite samples (Hovis and Roux, 1999). (Negatives of the heats of solution are plotted so that concave-down relationships represent positive enthalpies of mixing that “stand above” lines of ideal mixing on such a plot.) Although average reproducibility for the calorimetric data collected during the present study was good ( $\pm 0.4\%$ ), the necessity of utilizing 25 mg sample sizes for all but one composition resulted in lower precision (see Hovis and others, 1998) than is normal for this laboratory. The K-nepheline data of the current study have been fit to a quadratic function (solid curve of fig. 8) that relates the negatives of the heats of solution ( $-H_{soln}$ ) to composition ( $X_{K+Vac}$ ):

$$-H_{soln} \text{ (kJ/mol)} = 336.42 + 98.51 X_{K+Vac} - 109.20 X_{K+Vac}^2 \quad (8)$$

Because samples at  $X_{K+Vac}$  values of 0.572 and 0.639 show minor leucite X-ray peaks, it is necessary to evaluate the effect this might have had on the calorimetric data. One can write the following reaction for the breakdown of  $K_{0.875}[ ]_{0.125}Al_{0.875}Si_{1.125}$  kalsilite into Al:Si = 1:1 kalsilite plus leucite plus silica, respectively, as



TABLE 5  
*Solution calorimetric data*

Sample Number	Gram Formula Weight (g/mol)	Sample Weight (g)	Temperature Change During Dissolution (°C)	Mean Solution Temperature (°C)	Calorimeter Heat Capacity I Before Dissolution (J/deg)	Calorimeter Heat Capacity II After Dissolution (J/deg)	Heat of Solution I (from heat capacity before dissolution) (kJ/mol)	Heat of Solution II (from heat capacity after dissolution) (kJ/mol)
0805	142.5621	0.04509	0.029117	49.940	3880.8	3878.1	-356.56	-356.30
0805 *	142.5621	0.04544	0.029485	49.957	3873.8	3876.7	-357.63	-357.90
0705 *	143.3539	0.02669	0.017250	49.93	3861.5	3861.4	-357.05	-357.05
0705	143.3539	0.02424	0.015691	49.92	3868.0	3865.7	-358.22	-358.01
0704	144.3993	0.03904	0.025073	49.93	3866.6	3866.2	-357.88	-357.83
0704	144.3993	0.02775	0.017935	49.93	3868.4	3868.5	-360.30	-360.09
0704 *	144.3993	0.02656	0.017106	49.93	3861.9	3862.0	-358.44	-358.45
0716	145.4576	0.03004	0.019298	49.93	3867.1	3868.2	-360.64	-360.75
0716	145.4576	0.02656	0.017041	49.94	3865.7	3866.2	-360.06	-360.10
0716	145.4576	0.02656	0.016860	49.92	3866.9	3866.8	-356.33	-356.33
0707	146.5144	0.03648	0.022877	49.93	3863.3	3862.2	-354.25	-354.15
0707	146.5144	0.02668	0.016823	49.93	3865.3	3865.0	-356.38	-356.36
0707	146.5144	0.02566	0.016270	49.94	3866.0	3863.8	-358.20	-358.23
0709	147.5936	0.03583	0.022394	49.94	3864.0	3866.2	-355.73	-355.93
0717	147.5936	0.02551	0.015900	49.92	3867.8	3865.4	-355.09	-354.87
0717	147.5936	0.02550	0.015876	49.92	3865.0	3865.8	-354.46	-354.53
0717	147.5936	0.02478	0.015732	49.93	3866.1	3864.5	-361.54	-361.39

\* Experiment run in acid of the preceding experiment.



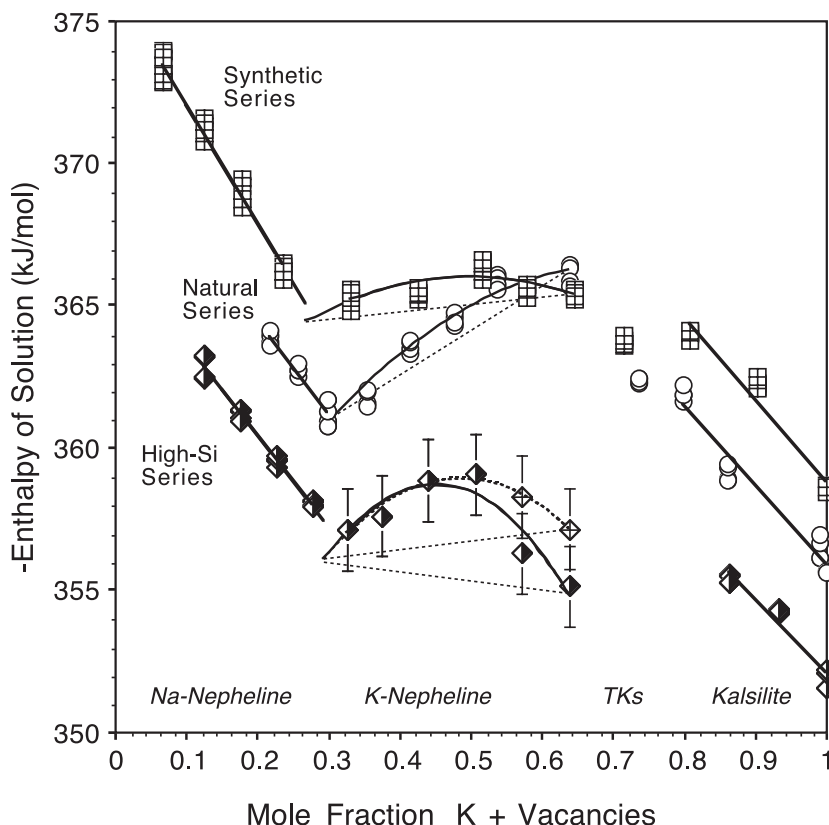


Fig. 8. Solution calorimetric data for three nepheline–kalsilite series. Data for the synthetic, natural, and high-Si series are shown by squares, circles, and diamonds, respectively. Data for K-nepheline specimens of the high-Si series are from the current investigation; error bars represent  $\pm 0.4\%$  of the heats of solution. Other data are from Hovis and Roux (1993, 1999). Note linear trends of the data at  $X_{K+Vac} < 0.25-0.30$ , then the change to concave-down relations for K-nepheline specimens (reflecting positive enthalpies of mixing), then the resumption of linear trends in the kalsilite data range. Alternate data points for the two most potassic K-nepheline specimens of the high-Si series represent maximum corrections for possible leucite contamination as discussed in the text. The dashed curve for high-Si K-nepheline specimens utilizes data for the three most sodic K-nephelines plus adjusted data for the other more potassic K-nephelines. Ideal mixing is represented as dashed lines that connect the Na- and K-rich ends of K-nepheline segments for each series. Names at the bottom of the plot give mineral designations over the appropriate compositional ranges; data are shown for two tetrakalsilite (TKs) samples, one each for the synthetic and natural series.

Using solution calorimetric data for Al:Si = 1:1 kalsilite (Hovis and Roux, 1993), leucite (unpublished data of this laboratory), and amorphous silica [data for  $\text{SiO}_2$  glass from Hovis (1984) were utilized, as there were no X-ray peaks corresponding to a  $\text{SiO}_2$  phase] it is estimated that the difference in the heat of solution between Na-free kalsilite having 12.5 mole percent excess Si ( $-351.8$  kJ/mol) and the three phases on the right side of equation (9) ( $-350.0$  kJ/mol) is only 1.8 kJ/mol. Adjusting the magnitude of calorimetric data for the two most potassic K-nepheline compositions by this amount (an approximation, as these specimens are not Na-free), one arrives at alternative heats of solution and a modified relationship shown as the dashed curve in figure 8:

$$-H_{\text{soln}} \text{ (kJ/mol)} = 340.58 + 75.28 X_{K+Vac} - 77.36 X_{K+Vac}^2 \quad (10)$$

The actual energetic effect is likely to be less than that shown in this figure, as breakdown is not complete, nor is there evidence that it involves the sodic component of the mineral. Small amounts of leucite, therefore, probably have only a small effect on the calorimetric data or on the enthalpies of mixing discussed next.

DISCUSSION

*Enthalpies of K-Na Mixing at 50 °C*

In interpreting both solvus and calorimetric data for the three nepheline–kalsilite series, it is critical to know alkali-site occupancies at the transition from Na-nepheline to K-nepheline. These can be determined through linear least-squares fits to unit-cell volume (or other cell parameters) within Na-nepheline and K-nepheline segments of the various series. Intersections of these lines give the compositions at which trends change. Moreover, plots against various compositional parameters such as  $X_K$ ,  $X_{K+Vac}$ ,  $X_{Na}$ , and  $X_{Na+Vac}$  (noting also that vacancies are constant across two of the three series) determine the  $X_{Na}$ ,  $X_K$ , and  $X_{Vac}$  contents at the transition. The resulting transitional compositions for all nepheline–kalsilite series are given in table 6.

From the data in table 6 one could conclude that the small alkali site of nepheline fills with  $Na^+$ ,  $Ca^{2+}$ , and vacancies before  $K^+$  enters that site. By the same token, the data demonstrate that it is possible for the large hexagonal alkali site to fill with  $K^+$  and vacancies before  $Na^+$  ( $\pm Ca^{2+}$ ) enters the site. Is one of these controls more important than the other? The work of Buerger and others (1954) and Barth (1963) both indicate preference of nepheline’s large alkali site by  $K^+$  and vacancies, and of the small site by  $Na^+$ . The work of Dollase and Thomas (1978) on silicic nepheline, however, further refines these observations by showing a large-site preference for vacancies; the authors interpret this to mean that  $Na^+$  is too small for the large hexagonal site. This interpretation could explain present data for the high-Si series, which shows  $K^+$  entry into nepheline’s large alkali site at a subpotassic composition ( $X_K = 0.17$ ) relative to  $X_K = 0.25$ . It is the large number of vacancies in high-Si samples, therefore, that could account for the seemingly premature  $K^+$  entry into the small alkali site (figs. 5, 6, and 7).

To calculate enthalpies of mixing for the various nepheline–kalsilite series the compositions given in table 6 have been utilized as the sodic end members of the K-nepheline segment for each series. Note that one member each of the natural (sample 8718;  $X_K = 0.215$ ,  $X_{Na+Ca} = 0.702$ ,  $X_{Vac} = 0.083$ ,  $X_{K+Vac} = 0.308$ ) and high-Si series (sample 9509;  $X_K = 0.152$ ,  $X_{Na} = 0.723$ ,  $X_{Vac} = 0.125$ ,  $X_{K+Vac} = 0.277$ ) is close in composition (within error) to the Na- to K-nepheline transitional compositions for those series ( $X_{K+Vac} = 0.306$  and  $0.272$ , respectively). For purposes of calorimetric data analysis these samples have been considered parts of both the Na- and K-nepheline compositional segments of the respective series. Quadratic polynomial expressions have been fit to the calorimetric data as a function of  $X_{K+Vac}$  from the

TABLE 6  
*Nepheline composition at the Na-Nepheline to K-Nepheline transition*

Series	Mole Percent	Mole Fraction	Mole Fraction	Mole Fraction	Mole Fraction	Mole Fraction
	Excess Si	K	Na ( $\pm Ca$ )	Vacancies	K+Vac	Na $\pm$ Ca+Vac
Synthetic Series	1.7%	0.251	0.732	0.017	0.268	0.749
Natural Series	5.2%	0.222	0.694	0.084	0.306	0.778
High-Si Series	12.5%	0.170	0.705	0.125	0.295	0.830

Compositions given are per 4 oxygen ions.

sodic to the potassic ends (taken to be near  $X_{K+Vac} \sim 0.64$ ) of the K-nepheline data ranges (fig. 8). The resulting curves show positive enthalpies of mixing that stand above the respective (dashed) lines of ideal mixing. Note, however, that magnitudes of the enthalpies of mixing are small for the synthetic and natural series. Moreover, magnitudes do not correlate well with critical temperatures of the three series. By comparison with K-Na feldspars (Hovis, 1988; Hovis and others, 1991) or muscovite–paragonite micas (Roux and Hovis, 1996), enthalpies of K-Na mixing of such low magnitude seem insufficient to generate the high critical temperatures seen in figures 3A and 3B.

Because immiscibility for nepheline–kalsilite involves coexistences between K-nepheline and a K-rich non-nepheline phase (see solvus figures in Sack and Ghiorso, 1998), it seems appropriate to analyze the solution calorimetric results across K-nepheline, tetrakalsilite, and kalsilite structural regions as a single data set. In order to allow for the possibility of asymmetric heats of mixing, third-order polynomial expressions have been utilized for the expanded compositional range. Note that this approach (fig. 9 and table 7) is imperfect in that it does not take into account possible energies associated with transformations among the various structures (probably

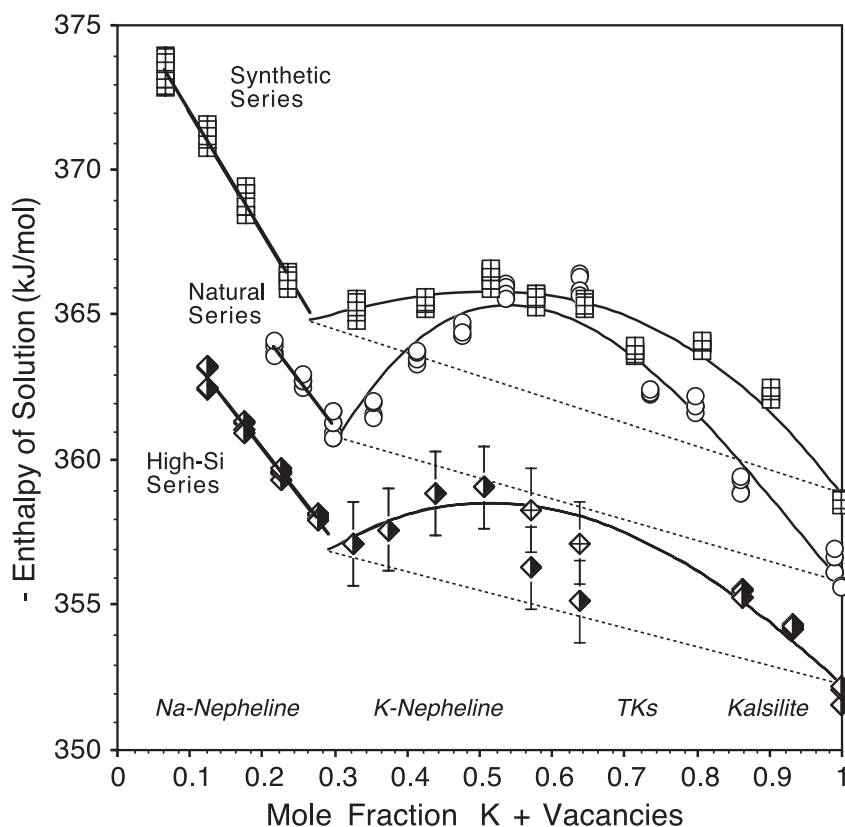


Fig. 9. An alternate interpretation of  $H_{ex}$  relative to figure 8. Solution calorimetric data for K-nepheline, tetrakalsilite, and kalsilite samples within each series are analyzed as a continuous data set. Leucite-corrected data are utilized for the two most potassic K-nepheline compositions of the high-Si series. Lines of ideal mixing connect data for Na-free kalsilite to compositions at which K (presumably) enters the small alkali site of nepheline (table 6). This analysis produces magnitudes for  $H_{ex}$  (fig. 10) that correlate well with the critical temperatures of the three solvi.

TABLE 7

Equations for K-nepheline, tetrakalsilite, and kalsilite calorimetric data of figure 9

Series	Coefficients to Equations			
	A0	A1	A2	A3
<i>Equations for calorimetric data</i>				
Synthetic Series	362.52	8.04	5.71	-17.46
Natural Series	336.31	122.54	-156.18	53.08
High-Si Series	348.46	41.85	-49.19	11.12
<i>Equations for lines of ideal mixing</i>				
Synthetic Series	366.92	-8.12		
Natural Series	362.89	-7.14		
High-Si Series	358.72	-6.49		

Equations for both the calorimetric data and lines of ideal mixing are for  $-H_{\text{soln}}$  (kJ/mol) expressed as power series using  $X_{\text{K+Vac}}$  as the compositional parameter. These apply to all data on the potassic side of the Na-nepheline to K-nepheline transition.

small). Nevertheless, the resulting enthalpies of mixing (fig. 10) display relative magnitudes that correlate positively with critical temperatures of the solvi, the highest  $T_c$  (natural series) associated with the greatest heats of mixing, and lower critical

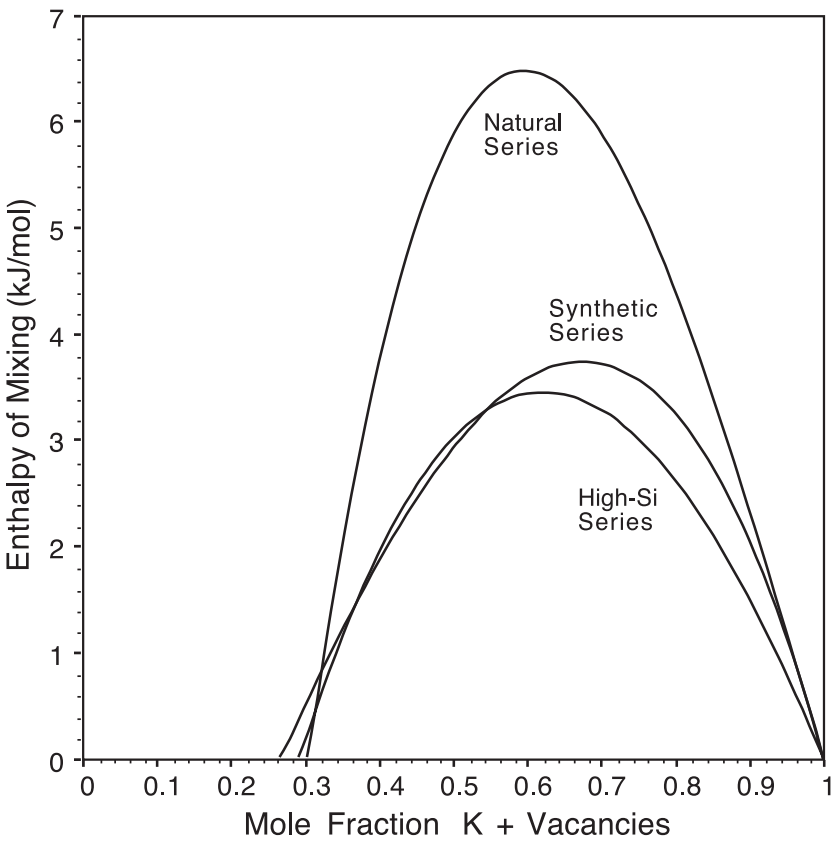


Fig. 10. Enthalpies of mixing for the three nepheline–kalsilite series based on analysis in figure 9 and equations in table 7.

temperatures linked to lower heats of mixing. Moreover, there is good correlation of the asymmetry of  $H_{\text{ex}}$  (fig. 10) with the critical composition of the natural-series solvus in that both are skewed toward more sodic compositions. So, although analysis of data across three structural regions (K-nepheline, tetrakalsilite, kalsilite) technically may not be rigorous, it does produce results for  $H_{\text{ex}}$  that sensibly connect thermodynamic data to phase equilibrium behavior.

#### *Crystal Chemistry and Thermodynamics*

Changes in the trends of the room-temperature unit-cell parameters shown in figures 5, 6 and 7 correlate well with the 50 °C solution calorimetric data of figure 8. Linear trends in the enthalpy relationships, and thus ideal thermodynamic behavior, are associated with one of two compositional regions, either  $X_{\text{K+Vac}} < 0.25$  or high  $X_{\text{K+Vac}}$  in the kalsilite data range. The former case is associated with vacancy =  $\text{K}^+$  substitution in the large hexagonal alkali site of nepheline. The latter case involves  $\text{Na}^+ = \text{K}^+$  substitution in the ditrigonal site of kalsilite. Linear behavior of the calorimetric data suggests that the substituting species comfortably fit into the structural positions involved, with no energetic indication of structural strain.

On the other hand, the entrance of  $\text{K}^+$  into the oval site of nepheline places a large ion into a relatively small site. This is accompanied by trends in the heats of solution that become curved and concave-down (fig. 8), reflecting positive enthalpies of mixing. One can interpret this as a reflection of structural strain.  $H_{\text{ex}}$  could be enhanced further by coexistence between nepheline and a non-nepheline potassic phase that contributes as well to the enthalpy relationships. Positive Gibbs energies of mixing ( $G_{\text{ex}}$ ) indeed are required for the presence of a solvus in mineral series that show complete solid solution (for example, alkali feldspars, Hovis and others, 1991). Positive enthalpies of mixing can be a major contributor to the latter:  $G_{\text{ex}} = H_{\text{ex}} - T S_{\text{ex}}$  (where  $S_{\text{ex}}$  is excess entropy).  $H_{\text{ex}}$  interpretations expressed in figures 9 and 10 are consistent with such a scenario.

The miscibility gaps measured in this and previous studies (Ferry and Blencoe, 1978; and Hovis and Crelling, 2000) correlate with alkali site occupancy. In all cases the sodic limbs of these gaps (figs. 3A and 3B) approach compositions of  $X_{\text{K}}$  and  $X_{\text{K+Vac}} \geq 0.25$ , not  $< 0.25$ . On the other hand, all solvi imply preference of the large alkali site for  $\text{K}^+$  alone at  $T \geq 500$  °C, leaving  $\text{Na}^+$  and vacancies to occupy the small oval site. This differs from room-T preference for vacancies by the hexagonal site determined from unit-cell data. Alkali-site occupancies, therefore, appear to change with temperature.

From a crystal chemical perspective the increasing amount of  $\text{K}^+$  in the hexagonal site with increased  $T$  could be attributed to abandonment of vacancy preference by the hexagonal site resulting from atomic vibration and diminishment in size distinction between  $\text{Na}^+$  and  $\text{K}^+$ . The increasing amount of  $\text{K}^+$  along the sodic limb of the solvus at  $T \geq 500$  °C can be attributed as well to vibrational mode, although at increasingly potassic compositions the small alkali site has little choice but to accept more  $\text{K}^+$ . Note that lower- $T$  compositional offsets among the sodic limbs of the various solvi (compare figs. 3A and 3B) are related to differences in vacancies, not  $\text{K}^+$ .

The potassic limbs of all three solvi coincide below 900 °C in figure 3A, and thus depend solely upon the  $\text{Na}^+$  content of the one and only ditrigonal alkali site of kalsilite. Linear behavior of the heats of solution in the kalsilite compositional region for all series (fig. 8) indicates ideal thermodynamic behavior. This suggests that the ditrigonal alkali site of kalsilite is unstrained by  $\text{Na}^+$  substitution.

#### *Variation in Critical Temperature*

The higher critical temperature (1265 °C) and relatively sodic critical composition of natural series samples correlate well with similar traits in  $H_{\text{ex}}$  shown in figure 9.

The crystal chemical explanation for these properties, however, is challenging. This behavior could be related to systematic decrease in the number of vacancies across the series imposed by  $[ ]\text{Ca}^{2+} = 2\text{K}^{+}$  substitution during ion-exchange synthesis. For every one  $\text{Ca}^{2+}$  that is replaced, two  $\text{K}^{+}$  ions enter the structure, one replacing the  $\text{Ca}^{2+}$  and another replacing a vacancy. This could account for the distinctly steeper trend in the heats of solution on the potassic side of the Na- to K-nepheline transition of the natural series relative to other series (figs. 8 and 9). Alternatively, the natural Monte Somma parent nepheline may have a more ordered Al-Si distribution than the two parent nepheline specimens hydrothermally synthesized from gel. Dollase and Thomas (1978) did indeed demonstrate a disordered Al-Si distribution in their synthetic high-Si nepheline sample. By analogy, natural feldspar samples are more ordered than their synthetic analogs, and K-Na mixing properties are greater against the backdrop of ordered than disordered Al-Si distributions (Hovis, 1988; Hovis and others, 1991). This is evidenced not only by feldspar heats of mixing (Hovis, 1988), but also by the critical temperatures of ordered (low albite-microcline) versus disordered (sanidine-analbite) feldspar solvi (Bachinski and Müller, 1971; Parsons, 1978). Still, the natural nepheline-kalsilite series has an Al:Si ratio of 0.948:1.052; considering the principle of Al-avoidance (Lowenstein, 1954) the potential for order/disorder relationships is considerably more limited than in the case of alkali feldspars, where Al:Si is 1:3. Additional uncertainty arises from the fact that little is known about how alkali-site K-Na-Ca-Vac distribution (or short-range order) in nepheline is affected by annealing temperature, cooling rate, and the temperature from which a sample is quenched.

The lower  $T_c$  (and  $H_{ex}$ ) of the high-Si series relative to the synthetic series could in part be related to the shortening of the K-Na substitutional range imposed by the presence of vacancies in 12.5 percent of the alkali sites. Just as the presence of An shortens the K-Na compositional span of an alkali feldspar series (Hovis, 1997; Hovis and Graeme-Barber, 1997), so does the presence of vacancies lessen the  $\text{K}^{+}\text{-Na}^{+}$  compositional range of a nepheline-kalsilite series, and thus the energetic consequences ( $H_{ex}$ ) of such substitution.

Excess entropy ( $S_{ex}$ ) also could play a role in lowering  $T_c$  in that  $S_{ex}$  acts in opposition to  $H_{ex}$  to lower  $G_{ex}$  ( $= H_{ex} - TS_{ex}$ ). No heat capacity data are available for our samples, so vibrational contributions to  $S_{ex}$  cannot be assessed. However, configurational entropies can be estimated by modeling site populations at room-temperature based on unit-cell data (for example, figs. 5, 6, and 7, table 6), not far from the temperature (50 °C) at which the solution calorimetric data were collected. Assuming that the large hexagonal site in nepheline prefers vacancies, calculations have been made across each nepheline-kalsilite series using the standard formulation  $-R \sum X_{is} \ln X_{is}$ , where  $R$  is the gas constant,  $X_{is}$  is the mole fraction of a species ( $i$ ) in a site ( $s$ ), and summation ( $\sum$ ) is made over all species in all sites. Excess configurational entropy ( $S_{con,ex}$ ) values were calculated using end-members defined by (1) the apparent composition at which K enters the small oval site of nepheline (table 6) and (2) Na-free kalsilite ( $X_{K+Vac} = 1$ ).  $G_{ex}$  was calculated by subtracting  $TS_{ex}$  (where  $T = 323.15$  K) from  $H_{ex}$  at each composition. Results of this exercise give maximum  $G_{ex}$  values of 1.6 kJ/mole for the synthetic series, 4.2 kJ/mol for the natural series, and 1.2 kJ/mole for the high-Si series (table 8). Correlation of the greatest  $G_{ex}$  with the highest  $T_c$  and lowest  $G_{ex}$  with lowest  $T_c$  is an encouraging result, even if  $G_{ex}$  values apply to 50 °C. Examination of the data in table 8 indicates that  $G_{ex}$  for the natural series is mostly a result of its greater  $H_{ex}$  relative to other series. On the other hand, the lowest  $G_{ex}$  of the high-Si series is affected to a greater extent by  $S_{con,ex}$  relative to modest values of  $H_{ex}$  for that series.

It also is possible that some or all of these crystalline solutions have short-range order, the presence of which would lower  $S_{ex}$  and raise  $T_c$ . The high  $G_{ex}$  of the natural



TABLE 8

*Maximum values of  $G_{ex}$  at  $\sim 50^\circ\text{C}$  with related  $H_{ex}$  and  $S_{ex}$  for three nepheline–kalsilite series*

Series	Maximum $G_{ex}$ (kJ/mol)	At $X_K$	At $X_{K+Vac}$	Accompanied by $H_{ex}$ (kJ/mol)	Accompanied by $-323.15 \cdot S_{con, ex}$ (kJ/mol)	Maximum $-323.15 \cdot S_{con, ex}$ (kJ/mol)
Synthetic Series	1.63	0.64	0.66	3.72	-2.09	-2.09
Natural Series	4.23	0.51	0.58	6.47	-2.24	-2.34
High-Si Series	1.17	0.48	0.60	3.43	-2.26	-2.32

series could imply that it has the lowest  $S_{ex}$  and thus the greatest degree of short-range effects. Likewise, a low  $G_{ex}$  for the high-Si series could imply a lesser degree of short-range order for that series. It is not known, however, whether such effects exist.

Finally, the applicability of these observations to conditions at the  $T_c$  of each series is unknown. As noted above,  $K^+$  appears to fill the hexagonal site at  $T \geq 500^\circ\text{C}$ , which implies that vacancies move to the oval alkali site at increased  $T$ . How this affects enthalpy and entropy, and to what degree these parameters might change with  $T$  is unknown. How calculations made for room-temperature and  $50^\circ\text{C}$  might apply to elevated  $T$  is unknown. It is interesting that the natural nepheline–kalsilite series, with its intermediate excess Si content, does display “intermediate behavior” in one sense, namely that the sodic limb of its solvus crosses that of the synthetic series at about  $800^\circ\text{C}$ , occupying an intermediate compositional position relative to the other series at the lowest temperature ( $500^\circ\text{C}$ ) of our solvus studies (figs. 3A and 3B).

Whatever the full explanation for the variation in  $T_c$  might be, the  $304^\circ\text{C}$  difference between the highest and lowest critical temperatures among the three series, as well as the variation in compositional width and asymmetry of the miscibility gaps, is impressive for excess-Si and Ca contents that vary only from 1.7 to 12.5 mole percent and 0 to 3.6 mole percent, respectively. In view of such data, as well as the possibility of order-disorder relationships and the potential overlay of these on mixing energies, it is not surprising that compositional scatter is considerable for naturally occurring solvus pairs in many mineral series.

#### SUMMARY AND CONCLUSIONS

The nepheline–kalsilite system serves as an excellent example of the interrelationships among mineral structure, crystal chemistry, thermodynamic properties, and phase equilibrium behavior. The structure of nepheline includes two crystallographically and topologically distinct alkali sites that can be occupied either by  $Na^+$ ,  $K^+$ , or vacancies. The presence of sites having distinctly different sizes in a mineral series where it is theoretically possible to have any proportion of K:Na has significant thermodynamic and phase equilibrium consequences. Entrance of  $K^+$  into the smaller alkali site in nepheline results in HF solution calorimetric data that show positive enthalpies of mixing for compositions on the K-rich side of the Na-nepheline to K-nepheline transition. This is accompanied by immiscibility in the form of coexisting mineral pairs. Positions of the sodic limbs of the solvi are governed in part by the preference of the large hexagonal alkali site for vacancies (rather than  $Na^+$ ) near room temperature, with an apparent switch in preference at  $T \geq 500^\circ\text{C}$ . Positions of the potassic limbs of the solvi are governed only by the substitution of relatively small  $Na^+$  into the ditrigonal site of kalsilite. The substitution of  $K^+$  into the hexagonal alkali site of nepheline produces little obvious strain, reflected by  $50^\circ\text{C}$  solution calorimetric data that indicate ideal or close-to-ideal thermodynamic behavior (fig. 8). Neverthe-

less, the collective structural (including possible order-disorder) and crystal chemical distinctions among these crystalline solutions produce contrasts in thermodynamic behavior and immiscibility that are impressive for the modest observed differences in system chemistry.

#### ACKNOWLEDGMENTS

This research was supported by the Earth Sciences Division of the National Science Foundation via grant EAR-0408829. It is a pleasure once again to acknowledge Professor Enrico Franco (Naples University), whose contribution of the Monte Somma nepheline specimen has benefited our research to a significant degree. We thank reviewers Michael Carpenter and C. M. B. Henderson for their constructive and helpful comments on this manuscript.

#### REFERENCES

- Bachinski, S. W., and Müller, G., 1971, Experimental Determinations of the Microcline–Low Albite Solvus: *Journal of Petrology*, v. 12, p. 329–356, doi:10.1093/petrology/12.2.329.
- Barth, T. F., 1963, The composition of nepheline: *Schweizerische Mineralogische und Petrographische Mitteilungen*, v. 43, p. 153–164.
- Benedetti, E., De Gennaro, M., and Franco, E., 1977, Primo rinvenimento in natura di tetrakalsilite: *Rendiconti Accademia Nazionale Lincei Series VIII*, v. 62, p. 835–838.
- Buerger, M. J., Klein, G. E., and Donnay, G., 1954, Determination of the crystal structure of nepheline: *American Mineralogist*, v. 39, p. 805–818.
- Capobianco, C., and Carpenter, M., 1989, Thermally induced changes in kalsilite (KAlSiO<sub>4</sub>): *American Mineralogist*, v. 74, p. 797–811.
- Carpenter, M. A., and Cellai, D., 1996, Microstructures and high-temperature phase transitions in kalsilite: *American Mineralogist*, v. 81, p. 561–584.
- Crelling, J. A., and Hovis, G. L., 1996, The significant effect of excess silicon on the nepheline–kalsilite solvus: *Geological Society of America Annual Meeting, Abstracts with Programs*, v. 28, p. A102–103.
- Dollase, W. A., and Freeborn, W. P., 1977, The structure of KAlSiO<sub>4</sub> with *P6<sub>3</sub>mc* symmetry: *American Mineralogist*, v. 62, p. 336–340.
- Dollase, W. A., and Peacor, D. R., 1971, Si–Al Ordering in Nephelines: *Contributions to Mineralogy and Petrology*, v. 30, p. 129–134, doi:10.1007/BF00372253.
- Dollase, W. A., and Thomas, W. M., 1978, The Crystal Chemistry of Silica-Rich, Alkali-Deficient Nepheline: *Contributions to Mineralogy and Petrology*, v. 66, p. 311–318, doi:10.1007/BF00373415.
- Donnay, G., Schairer, J. F., and Donnay, J. D. H., 1959, Nepheline solid solutions: *Mineralogical Magazine*, v. 32, p. 93–109, doi:10.1180/minmag.1959.32.245.02.
- Ferry, J. M., and Blencoe, J. G., 1978, Subsolidus phase relations in the nepheline–kalsilite system at 0.5, 2.0, and 5.0 kbar: *American Mineralogist*, v. 63, p. 1225–1240.
- Hahn, T., and Buerger, M. J., 1955, The detailed structure of nepheline, KNa<sub>3</sub>Al<sub>4</sub>Si<sub>4</sub>O<sub>16</sub>: *Zeitschrift für Kristallographie*, v. 106, p. 308–338.
- Hamilton, D. L., and Henderson, C. M. B., 1968, The preparation of silicate compositions by a gelling method: *Mineralogical Magazine*, v. 36, p. 832–838, doi:10.1180/minmag.1968.036.282.11.
- Hamilton, D. L., and MacKenzie, W. S., 1960, Nepheline Solid Solution in the System NaAlSiO<sub>4</sub>–KAlSiO<sub>4</sub>–SiO<sub>2</sub>: *Journal of Petrology*, v. 1, p. 56–72, doi:10.1093/petrology/1.1.56.
- Henderson, C. M. B., and Gibb, F. G. F., 1983, Felsic mineral crystallization trends in differentiating alkaline basic magmas: *Contributions to Mineralogy and Petrology*, v. 84, p. 355–364, doi:10.1007/BF01160287.
- Hippeler, B., and Bohm, H., 1989, Structure investigation of sodium nephelines: *Zeitschrift für Kristallographie*, v. 187, p. 39–53.
- Holland, T. J. B., and Redfern, S. A. T., 1997, Unit cell refinement from powder diffraction data: the use of regression diagnostics: *Mineralogical Magazine*, v. 61, p. 65–77.
- Hovis, G. L., 1984, A hydrofluoric acid solution calorimetric investigation of glasses in the systems NaAlSi<sub>3</sub>O<sub>8</sub>–KAlSi<sub>3</sub>O<sub>8</sub> and NaAlSi<sub>3</sub>O<sub>8</sub>–Si<sub>4</sub>O<sub>8</sub>: *Geochimica et Cosmochimica Acta*, v. 48, p. 523–525, doi:10.1016/0016-7037(84)90280-1.
- 1988, Enthalpies and volumes related to K–Na mixing and Al–Si order/disorder in alkali feldspars: *Journal of Petrology*, v. 29, p. 731–763, doi:10.1093/petrology/29.4.731.
- 1997, Hydrofluoric acid solution calorimetric investigation of the effect of anorthite component on enthalpies of K–Na mixing in feldspars: *American Mineralogist*, v. 82, p. 149–157.
- Hovis, G. L., and Crelling, J. A., 2000, The effects of excess silicon on immiscibility in the nepheline–kalsilite system: *American Journal of Science*, v. 300, p. 238–249.
- Hovis, G. L., and Graeme-Barber, A., 1997, Volumes of K–Na mixing for low albite–microcline crystalline solutions at elevated temperature: A test of regular solution thermodynamic models: *American Mineralogist*, v. 82, p. 158–164.
- Hovis, G. L., and Roux J., 1993, Thermodynamic mixing properties of nepheline–kalsilite crystalline, solutions: *American Journal of Science*, v. 293, p. 1108–1127.

- 1999, Thermodynamics of excess silicon in nepheline and kalsilite crystalline solutions: *European Journal of Mineralogy*, v. 11, p. 815–827.
- Hovis, G. L., Delbove, F., and Bose, M. R., 1991, Gibbs energies and entropies of K-Na mixing for alkali feldspars from phase equilibrium data: Implications for feldspar solvi and short-range order: *American Mineralogist*, v. 76, p. 913–927.
- Hovis, G. L., Spearing, D. R., Stebbins, J. F., Roux, J., and Clare, A., 1992, X-ray powder diffraction and  $^{23}\text{Na}$ ,  $^{27}\text{Al}$ , and  $^{29}\text{Si}$  MAS-NMR investigation of nepheline–kalsilite crystalline solutions: *American Mineralogist*, v. 77, p. 19–29.
- Hovis, G. L., Roux, J., and Richet, P., 1998, A new era in hydrofluoric acid solution calorimetry: Reduction of required sample size below ten milligrams: *American Mineralogist*, v. 83, p. 931–934.
- Hovis, G. L., Crelling, J., Wattles, D., Dreibelbis, B., Dennison, A., Keohane, M., and Brennan, S., 2003, Thermal expansion of nepheline–kalsilite crystalline solutions: *Mineralogical Magazine*, v. 67, p. 535–546, doi:10.1180/0026461036730115.
- Hovis, G. L., Person, E., Spooner, A., and Roux, J., 2006, Thermal expansion of highly silicic nepheline–kalsilite crystalline solutions: *Mineralogical Magazine*, v. 70, p. 383–396, doi:10.1180/0026461067040339.
- Lowenstein, W., 1954, The distribution of aluminum in the tetrahedra of silicates and aluminates: *American Mineralogist*, v. 39, p. 92–96.
- Merlino, S., 1984, Feldspathoids: Their average and real structures, in Brown, W. L., editor, *Feldspars and feldspathoids*: Dordrecht, Reidel Publishing Company, p. 435–470.
- Nitkiewicz, A. M., Kerrick, D., and Hemingway, B. S., 1983, The effect of particle size on enthalpy of solution of quartz: *Geological Society of America Annual Meeting, Abstracts with Programs*, v. 15, p. 653.
- Parsons, I., 1978, Alkali feldspar: Which solvus?: *Physics and Chemistry of Minerals*, v. 2, p. 199–213, doi:10.1007/BF00308173.
- Perrotta, A. J., and Smith, J. V., 1965, The crystal structure of kalsilite  $\text{KAlSiO}_4$ : *Mineralogical Magazine*, v. 35, p. 588–595, doi:10.1180/minmag.1965.035.272.02.
- Roux, J., and Hovis, G. L., 1996, Thermodynamic mixing models for muscovite–paragonite solutions based on solution calorimetric and phase equilibrium data: *Journal of Petrology*, v. 37, p. 1241–1254, doi:10.1093/petrology/37.5.1241.
- Sack, R. O., and Ghiorso, M. S., 1998, Thermodynamics of feldspathoid solutions: *Contributions to Mineralogy and Petrology*, v. 130, p. 256–274, doi:10.1007/s004100050364.
- Smith, J. V., and Tuttle, O. F., 1957, The nepheline–kalsilite system: I. X-ray data for the crystalline phases: *American Journal of Science*, v. 255, p. 282–305.
- Stebbins, J. F., Murdoch, J. B., Carmichael, I. S. E., and Pines, A., 1986, Defects and Short-range Order in Nepheline Group Minerals: a Silicon-29 Nuclear Magnetic Resonance Study: *Physics and Chemistry of Minerals*, v. 13, p. 371–381, doi:10.1007/BF00309182.
- Thompson, J. B., Jr., and Waldbaum, D. R., 1969a, Analysis of the two-phase region halite–sylvite in the system  $\text{NaCl-KCl}$ : *Geochimica et Cosmochimica Acta*, v. 33, p. 671–690, doi:10.1016/0016-7037(69)90114-8.
- 1969b, Mixing properties of sanidine crystalline solutions: III. Calculations based on two-phase data: *American Mineralogist*, v. 54, p. 811–838.
- Tuttle, O. F., and Smith, J. V., 1958, The nepheline–kalsilite system: II. Phase relations: *American Journal of Science*, v. 256, p. 571–589.
- Waldbaum, D. R., and Robie, R. A., 1970, An internal sample container for hydrofluoric acid solution calorimetry: *Journal of Geology*, v. 78, p. 736–741.